Glucocorticoids exacerbate obesity and insulin resistance in neuron-specific proopiomelanocortin-deficient mice

James L. Smart,[1] Virginie Tolle,[1] and Malcolm J. Low[1,2,3]

[1]Vollum Institute, [2]Department of Behavioral Neuroscience, and [3]Center for the Study of Weight Regulation and Associated Disorders, Oregon Health & Science University, Portland, Oregon, USA.

Null mutations of the proopiomelanocortin gene (*Pomc*$^{-/-}$) cause obesity in humans and rodents, but the contributions of central versus pituitary POMC deficiency are not fully established. To elucidate these roles, we introduced a POMC transgene (*Tg*) that selectively restored peripheral melanocortin and corticosterone secretion in *Pomc*$^{-/-}$ mice. Rather than improving energy balance, the genetic replacement of pituitary POMC in *Pomc*$^{-/-}$*Tg*$^{+}$ mice aggravated their metabolic syndrome with increased caloric intake and feed efficiency, reduced oxygen consumption, increased subcutaneous, visceral, and hepatic fat, and severe insulin resistance. Pair-feeding of *Pomc*$^{-/-}$*Tg*$^{+}$ mice to the daily intake of lean controls normalized their rate of weight gain but did not abolish obesity, indicating that hyperphagia is a major but not sole determinant of the phenotype. Replacement of corticosterone in the drinking water of *Pomc*$^{-/-}$ mice recapitulated the hyperphagia, excess weight gain and fat accumulation, and hyperleptinemia characteristic of genetically rescued *Pomc*$^{-/-}$*Tg*$^{+}$ mice. These data demonstrate that CNS POMC peptides play a critical role in energy homeostasis that is not substituted by peripheral POMC. Restoration of pituitary POMC expression to create a de facto neuronal POMC deficiency exacerbated the development of obesity, largely via glucocorticoid modulation of appetite, metabolism, and energy partitioning.

Introduction

Deciphering the complex regulatory mechanisms for energy balance is a health-care priority because of the rapidly growing prevalence of obesity (1). Energy homeostasis is enabled by peripheral signals informing the CNS about energy storage levels and metabolic status. Vagal afferents and hormones including leptin, insulin, ghrelin, and glucocorticoids relay this interoceptive information to hypothalamic and brainstem nuclei that in turn regulate energy consumption, utilization, and storage (2, 3). Peripheral information processed centrally is used to elicit appropriate feeding, endocrine, and autonomic motor responses.

Neurons in the arcuate nucleus of the hypothalamus that express the gene encoding proopiomelanocortin (POMC) play a major role in this physiological network (4–6). Genetic disruption of either the mouse *Pomc* or the human *POMC* gene causes early-onset obesity (7–9), suggesting that endogenous POMC pathways are essential for the regulation of energy homeostasis. POMC is processed posttranslationally to the endogenous opioid β-endorphin and the melanocortin peptides ACTH, α-melanocyte-stimulating hormone (αMSH), βMSH, and γMSH. Absence of some or all of these peptides could potentially contribute to the obesity syndrome. In the CNS, energy balance is profoundly modulated by the anorexigenic peptide αMSH via melanocortin receptor-4 (MC4-R) activation. Central administration of αMSH (10, 11) or a synthetic analog, MTII (12, 13), reduces food intake in rodents. Conversely, mutations of MC4-R, the most abundant melanocortin receptor in the CNS, lead to obesity in humans and mice (14–21). MC4-R is also a target for agouti-related protein (AGRP), a naturally occurring receptor antagonist released from terminals of neuropeptide Y/AGRP arcuate nucleus neurons that parallel the distribution of POMC fibers throughout the limbic system (22). The less abundant MC3-R appears to play a distinct role from activation of MC4-R in energy homeostasis (23, 24). Furthermore, β-endorphin has independent modulatory effects on appetite, satiety, and food reinforcement in the brain's reward circuitry (25, 26).

Intermediate lobe pituitary melanotrophs are the major source of circulating αMSH, although the importance of peripheral αMSH in energy homeostasis is unclear. Anterior lobe corticotrophs secrete ACTH that stimulates the production of glucocorticoids from the adrenals. Therefore, a disruption in pituitary POMC function could impact energy balance secondarily via altered levels of glucocorticoid hormones, which regulate metabolism, fat distribution, and the development of obesity independently of αMSH (3). Corticosterone is known to play a permissive role in rodents for positive energy balance. Adrenalectomy normalizes several metabolic abnormalities observed in rodents with monogenic obesity syndromes, and the effects of adrenalectomy can be reversed by glucocorticoid replacement (27–32). Furthermore, chronic hypersecretion of cortisol associated with Cushing syndrome is associated with altered fat distribution and visceral obesity (33).

While the majority of energy homeostasis studies have focused on CNS POMC, a requirement for pituitary POMC peptides, either directly through peripheral actions of melanocortins (34) or indirectly via glucocorticoids, has not been established conclusively. Here, we compare *Pomc*$^{-/-}$ mice with a global deficiency of POMC with a compound mutant strain of *Pomc*$^{-/-}$*Tg*$^{+}$ mice with a neuron-specific deficiency of POMC to differentiate the roles played by central and peripheral POMC peptides in the control of feeding and metabolism.

Nonstandard abbreviations used: HPA, hypothalamic-pituitary-adrenal; MC4-R, melanocortin receptor-4; MSH, melanocyte-stimulating hormone; POMC, proopiomelanocortin; RQ, respiratory quotient.

Conflict of interest: The authors have declared that no conflict of interest exists.

Citation for this article: *J. Clin. Invest.* **116**:495–505 (2006). doi:10.1172/JCI25243.

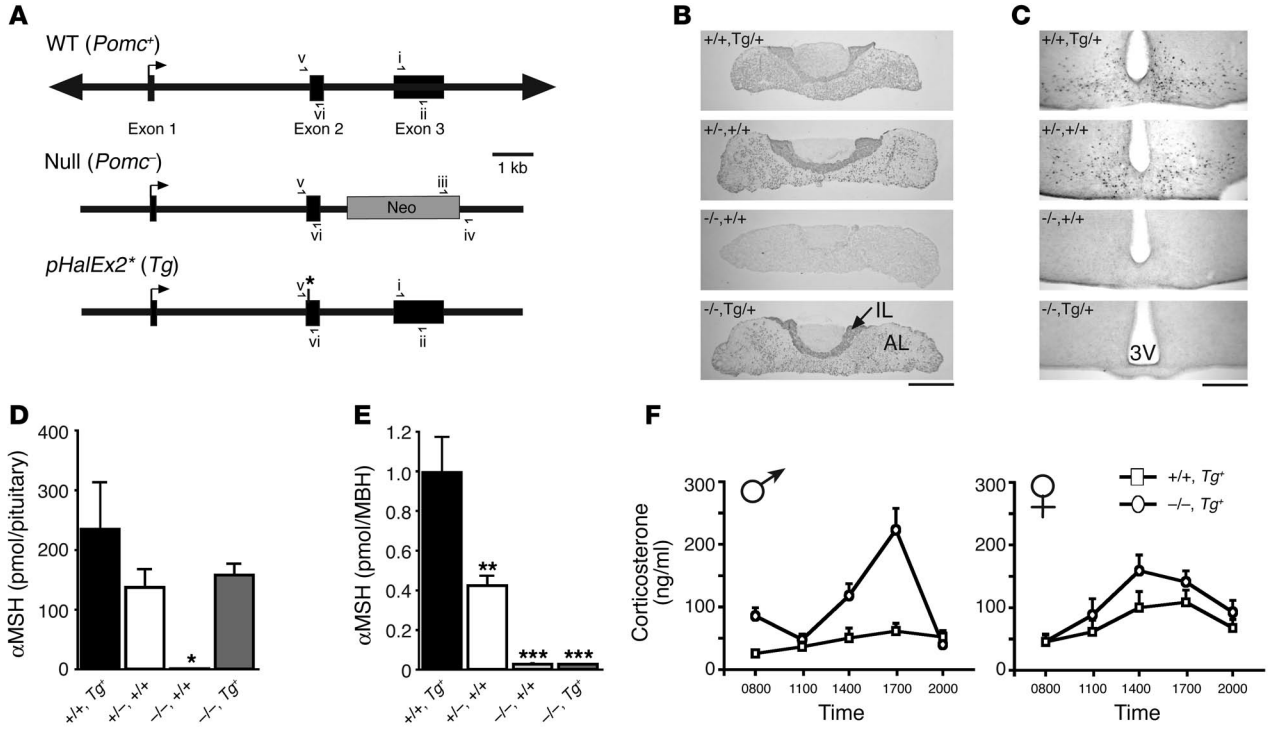

Figure 1
Transgenic rescue of pituitary POMC expression. (**A**) Schematic of WT *Pomc*$^+$, null *Pomc*$^-$, and *pHalEx2* Tg* alleles. A neomycin (*Neo*) selection cassette replaces exon 3 in the *Pomc*$^-$ allele, and a 23-bp oligonucleotide (asterisk) is inserted in the 5′ untranslated region of exon 2 of the *Tg* allele. The arrow above exon 1 represents the transcriptional start site. PCR primer locations for genotyping of the *Pomc*$^+$ (i and ii), *Pomc*$^-$ (iii and iv), and *Tg* (v and vi) alleles are indicated by half-arrows. (**B** and **C**) ACTH immunoreactivity in the pituitary anterior lobe (AL), intermediate lobe (IL), and medial basal hypothalamus (MBH) from mice of the indicated genotypes. 3V, third ventricle. Scale bars: 300 μm (pituitary) and 100 μm (MBH). (**D** and **E**) Quantitation of αMSH content in the pituitary gland and MBH from male mice of the indicated genotypes ($n = 4$). *$P < 0.01$, **$P < 0.001$, and ***$P < 0.0001$ compared with *Pomc*$^{+/+}$*Tg*$^+$. (**F**) Basal diurnal corticosterone levels in 10- to 15-week-old male and female *Pomc*$^{+/+}$*Tg*$^+$ and *Pomc*$^{-/-}$*Tg*$^+$ mice.

Results

Transgenic rescue of pituitary POMC in Pomc$^{-/-}$ *mice*. Transgenic mice were generated with a modified genomic construct predicted to express POMC in pituitary cells but not neurons (35, 36). The *Pomc* WT (*Pomc*$^+$), KO (*Pomc*$^-$), and *pHalEx2** transgenic (*Tg*) alleles are depicted schematically in Figure 1A. Hemizygous *Tg*$^+$ transgenic mice were intercrossed to *Pomc*$^{+/-}$ mice to generate *Pomc*$^{+/-}$*Tg*$^+$ breeders. *Pomc*$^{+/-}$*Tg*$^+$ females were subsequently bred with either *Pomc*$^{+/+}$ or *Pomc*$^{-/-}$ males to generate *Pomc*$^{+/+}$, *Pomc*$^{+/-}$, and *Pomc*$^{-/-}$ mice with or without the transgene (*Tg*$^+$ or +/+, respectively).

Immunohistochemical detection of ACTH (Figure 1, B and C) or β-endorphin (data not shown) confirmed tissue-specific expression of the *pHalEx2** transgene with restoration of peptide immunoreactivity in the pituitary anterior and intermediate lobes (Figure 1B) but not the hypothalamus (Figure 1C) of *Pomc*$^{-/-}$*Tg*$^+$ mice. Fully processed αMSH (ACTH 1-13-amide) was quantified by RIA of tissue extracts (Figure 1, D and E). Hypothalamic αMSH was reduced by 50% in *Pomc*$^{+/-}$ mice and was undetectable in both *Pomc*$^{-/-}$ and *Pomc*$^{-/-}$*Tg*$^+$ mice. Pituitary αMSH was undetectable only in *Pomc*$^{-/-}$ mice but was similarly high (100–200 pmol per pituitary) in the other genotypes, including the *Pomc*$^{-/-}$*Tg*$^+$ mice. Furthermore, plasma levels of αMSH in *Pomc*$^{-/-}$*Tg*$^+$ mice were restored to the normal range of *Pomc*$^{+/+}$*Tg*$^+$ mice (54 ± 42 versus 48 ± 35 fmol/ml, respectively).

Plasma corticosterone levels were measured in 10- to 15-week-old mice at 3-hour intervals from 0800 to 2000 hours (Figure 1F) to assess the effects of genetically restored pituitary expression of ACTH on the hypothalamic-pituitary-adrenal (HPA) axis. *Pomc*$^{+/+}$*Tg*$^+$ mice exhibited the WT diurnal rhythm of corticosterone secretion with a nadir early in the light phase and increasing levels before the onset of darkness. Female *Pomc*$^{+/+}$*Tg*$^+$ mice had higher peak corticosterone values than males, reflecting the normal sexual dimorphism of the HPA axis. *Pomc*$^{-/-}$ mice of both sexes had undetectable corticosterone at all time points. Female *Pomc*$^{-/-}$*Tg*$^+$ mice retained a diurnal pattern of corticosterone secretion with normal basal and only modestly increased peak values. In contrast, male *Pomc*$^{-/-}$*Tg*$^+$ mice exhibited an altered pattern of corticosterone secretion with exaggerated nadir and peak levels. *pHalEx2** transgene expression did not alter corticosterone levels in the *Pomc*$^{+/-}$ background (data not shown).

Long-term effects of pituitary POMC rescue in Pomc$^{-/-}$ *mice on growth, adipose mass, and glucose homeostasis*. The complete absence of POMC in *Pomc*$^{-/-}$ mice resulted in significantly increased body weight in both sexes compared with that of *Pomc*$^{+/+}$ mice, while haploinsufficiency in *Pomc*$^{+/-}$ mice produced a more subtle intermediate phenotype evident primarily in males (Figure 2A). Expression of the *pHalEx2** transgene had no effect on weight gain in either *Pomc*$^{+/+}$*Tg*$^+$ or *Pomc*$^{+/-}$*Tg*$^+$ mice. In con-

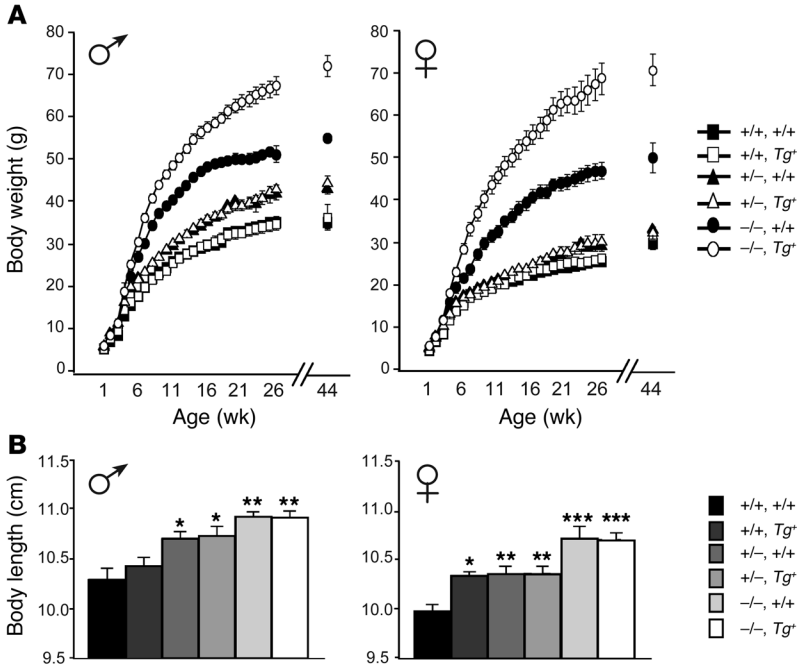

Figure 2
The effects of rescued pituitary POMC expression on body weight and length in the *Pomc*$^{-/-}$ background. (**A**) Body weight curves for male and female *Pomc*$^{+/+}$, *Pomc*$^{+/-}$, and *Pomc*$^{-/-}$ mice with and without the *pHalEx2** transgene (n = 9–44). Repeated-measures ANOVAs from 1 to 26 weeks old showed interactions between week and genotype for both sexes. Males: $P < 0.0001$, *Pomc*$^{-/-}$, *Pomc*$^{-/-}$*Tg*$^{+}$, and *Pomc*$^{+/-}$*Tg*$^{+}$ compared with *Pomc*$^{+/+}$ or *Pomc*$^{+/+}$*Tg*$^{+}$; $P < 0.001$, *Pomc*$^{+/-}$ compared with *Pomc*$^{+/+}$ or *Pomc*$^{+/+}$*Tg*$^{+}$. Females: $P < 0.0001$, *Pomc*$^{-/-}$ and *Pomc*$^{-/-}$*Tg*$^{+}$ compared with *Pomc*$^{+/+}$ or *Pomc*$^{+/+}$*Tg*$^{+}$. (**B**) Body lengths of males at age 44 ± 1.3 weeks and females at age 59 ± 2 weeks differed by genotype ($F_{5,44} = 5.9$, $P < 0.0005$, and $F_{5,37} = 13.4$, $P < 0.0001$, respectively). *$P < 0.01$, **$P < 0.001$, and ***$P < 0.0001$ compared with *Pomc*$^{+/+}$.

trast, restoration of peripheral POMC expression in *Pomc*$^{-/-}$*Tg*$^{+}$ mice markedly augmented weight gain compared with all other genotypes. As early as age 4 weeks, *Pomc*$^{-/-}$*Tg*$^{+}$ mice weighed significantly more than *Pomc*$^{-/-}$ mice. By age 26 weeks, male and female *Pomc*$^{-/-}$*Tg*$^{+}$ mice had gained 30% and 40% more weight, respectively, than their *Pomc*$^{-/-}$ siblings. Increased body weight was partially due to increased linear growth in *Pomc*$^{+/-}$ and *Pomc*$^{-/-}$ mice of both sexes (Figure 2B). However, the *pHalEx2** transgene did not further alter body length in these animals, indicating that it was the loss of CNS and not pituitary POMC peptides that directly or indirectly accentuated linear growth in *Pomc* mutants.

Altered lipid accumulation in both intra-abdominal and subcutaneous fat depots was responsible for most of the differences in body weight among genotypes (Figure 3). Renal, visceral, gonadal, and subcutaneous inguinal fat pads were all significantly heavier in *Pomc*$^{-/-}$ compared with *Pomc*$^{+/+}$ or *Pomc*$^{+/+}$*Tg*$^{+}$ mice, with the largest increase occurring in gonadal fat. *Pomc*$^{-/-}$*Tg*$^{+}$ mice had further increases in the mass of renal, visceral, and inguinal white fat pads, with a disproportionately greater change in inguinal fat (data shown for females only). Interestingly, the gonadal fat pads of male *Pomc*$^{-/-}$*Tg*$^{+}$ mice were similar in weight to those of *Pomc*$^{+/+}$ siblings and smaller than those of *Pomc*$^{-/-}$ siblings for either sex despite large increases in all other adipose depots. Liver mass was also substantially increased with prominent steatosis in *Pomc*$^{-/-}$*Tg*$^{+}$ mice. Consistent with their elevated body weights, heterozygous *Pomc*$^{+/-}$ and *Pomc*$^{+/-}$*Tg*$^{+}$ males displayed modest increases in fat pad and liver mass.

Fasting blood glucose and insulin levels were obtained at age 6–8 months (Table 1). Male *Pomc*$^{-/-}$ and *Pomc*$^{-/-}$*Tg*$^{+}$ mice exhibited significantly elevated fasting glucose levels. However, only *Pomc*$^{-/-}$*Tg*$^{+}$ mice of both sexes had significantly elevated fasting insulin levels compared with all other genotypes. The homeostasis assessment (HOMA) index was calculated to estimate the magnitude of insulin resistance (Table 1), and a 2-factor ANOVA demonstrated highly significant main effects of genotype ($F_{5,110} = 24.4$, $P < 0.0001$) and sex ($F_{1,110} = 26.9$, $P < 0.0001$, male > female) but no interaction between the 2 variables. In parallel to their insulin levels, *Pomc*$^{-/-}$

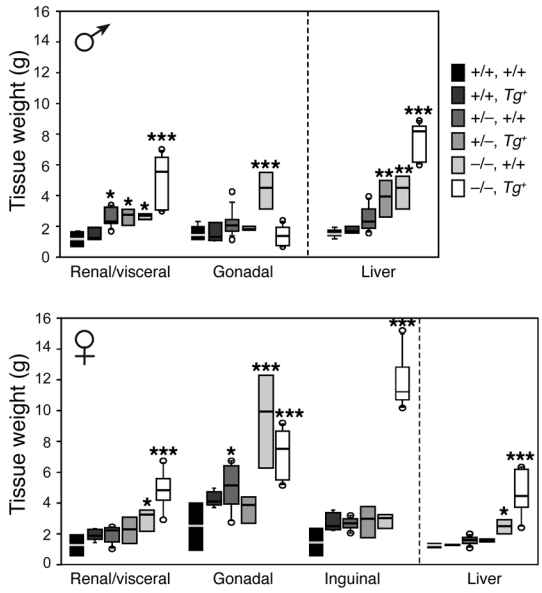

Figure 3
Weights of adipose tissue and liver from male and female *Pomc*$^{+/+}$, *Pomc*$^{+/-}$, and *Pomc*$^{-/-}$ mice with and without *pHalEx2** transgene expression. Adipose depots are the combined renal/visceral, gonadal, and subcutaneous inguinal white fat pads. The box and whisker plots show the 10th, 25th, 50th (median), 75th, and 90th percentiles and individual outlying data points (open circles). Males, age 41 ± 1 weeks (n = 3–10). Females, age 55 ± 1.7 weeks (n = 4–6). *$P < 0.05$, **$P < 0.01$, and ***$P < 0.0001$ compared with *Pomc*$^{+/+}$.

Table 1
Glucose homeostasis in WT and mutant *Pomc* mice

	Male			Female		
Genotype	**Glucose (mg/dl)**	**Insulin (ng/ml)**	**HOMA index**	**Glucose (mg/dl)**	**Insulin (ng/ml)**	**HOMA index**
Pomc$^{+/+}$	89 ± 7	0.73 ± 0.20	4.7 ± 1.8	83 ± 5	0.46 ± 0.08	2.7 ± 0.6
Pomc$^{+/+}$*Tg*$^{+}$	94 ± 8	0.99 ± 0.30	6.5 ± 2.4	78 ± 6	0.60 ± 0.20	3.6 ± 1.6
Pomc$^{+/-}$	108 ± 7	0.86 ± 0.14	6.1 ± 1.0	85 ± 6	0.36 ± 0.03	1.9 ± 0.2
Pomc$^{+/-}$*Tg*$^{+}$	102 ± 9	1.38 ± 0.20	9.6 ± 1.9	88 ± 7	0.32 ± 0.06	1.8 ± 0.3
Pomc$^{-/-}$	124 ± 8^{A}	1.15 ± 0.17	8.9 ± 1.1	85 ± 13	0.78 ± 0.33	4.6 ± 2.2
Pomc$^{-/-}$*Tg*$^{+}$	125 ± 13^{A}	2.91 ± 0.54^{B}	26.5 ± 6.5^{B}	89 ± 6	2.52 ± 0.33^{B}	14.8 ± 2.4^{B}

Fasting glucose and insulin levels were from 6- to 8-month-old mice (n = 5–23). The homeostasis assessment (HOMA) index of insulin resistance was calculated using the formula [blood glucose (mmol/l)][plasma insulin (mU/l)]/22.5. $^{A}P < 0.01$ versus *Pomc*$^{+/+}$ and *Pomc*$^{+/+}$*Tg*$^{+}$; $^{B}P < 0.0001$ versus all other genotypes.

Tg^{+} mice had increased HOMA values ($P < 0.0001$ compared with each other genotype), while the index in glucocorticoid-deficient *Pomc*$^{-/-}$ mice was only marginally different from that in *Pomc*$^{+/+}$ or *Pomc*$^{+/-}$ mice ($P < 0.05$ for both comparisons).

Development and maintenance of obesity in young and adult Pomc$^{-/-}$ *and* Pomc$^{-/-}$Tg^{+} *mice were due to distinct combinations of altered food intake and metabolic rate*. Our initial characterization studies involved all 6 possible genotypes of compound mutant mice and revealed a relatively mild phenotype in male *Pomc*$^{+/-}$ mice and no effect of *pHalEx2* Tg* expression on energy balance in the *Pomc*$^{+/+}$ or *Pomc*$^{+/-}$ genetic background. Therefore, we limited our follow-up studies with additional cohorts of mice to the 3 most informative genotypes that could also be generated by a more efficient breeding strategy: *Pomc*$^{-/-}$ and *Pomc*$^{-/-}$*Tg*$^{+}$ experimental groups and a *Pomc*$^{+/+}$*Tg*$^{+}$ control group.

At age 6 weeks, *Pomc*$^{-/-}$ and *Pomc*$^{-/-}$*Tg*$^{+}$ mice were hyperphagic and consumed 25% and 60% more food, respectively, over 24 hours compared with *Pomc*$^{+/+}$*Tg*$^{+}$ controls (Figure 4A). In contrast, by age 26 weeks, there was no longer a measurable difference in 24-hour food intake between *Pomc*$^{-/-}$ and *Pomc*$^{+/+}$*Tg*$^{+}$ mice, although *Pomc*$^{-/-}$*Tg*$^{+}$ mice remained overtly hyperphagic at essentially the same level exhibited at age 6 weeks (Figure 4B). After normalization of food intake to estimated metabolic mass with the scaling formula described by Pace et al. (37), *Pomc*$^{-/-}$ and *Pomc*$^{-/-}$*Tg*$^{+}$ mice remained hyperphagic compared with their *Pomc*$^{+/+}$*Tg*$^{+}$ siblings at age 6 weeks (Figure 4C). However, by age 9 weeks, all genotypes consumed the same quantity of food relative to their estimated metabolic mass. Despite continued increases in body weight over time, the absolute daily food intake for each genotype remained essentially constant between ages 9 and 26 weeks. Consequently, normalized food intake continued to decrease and was actually significantly lower in all POMC-deficient mice compared with their *Pomc*$^{+/+}$*Tg*$^{+}$ control siblings at age 26 weeks (Figure 4C). This trend was more pronounced in *Pomc*$^{-/-}$ than in *Pomc*$^{-/-}$*Tg*$^{+}$ mice.

To explain the maintenance of obesity in the mutant mice in the context of their measured drop in either absolute or normalized caloric intake, we assessed basal metabolic rates by indirect calorimetry. VO_2 was measured during the animals' least active phase of the diurnal light-dark cycle and expressed relatively to estimated metabolic mass using the scaling formula. At age 10 weeks, when body weights were relatively more similar among

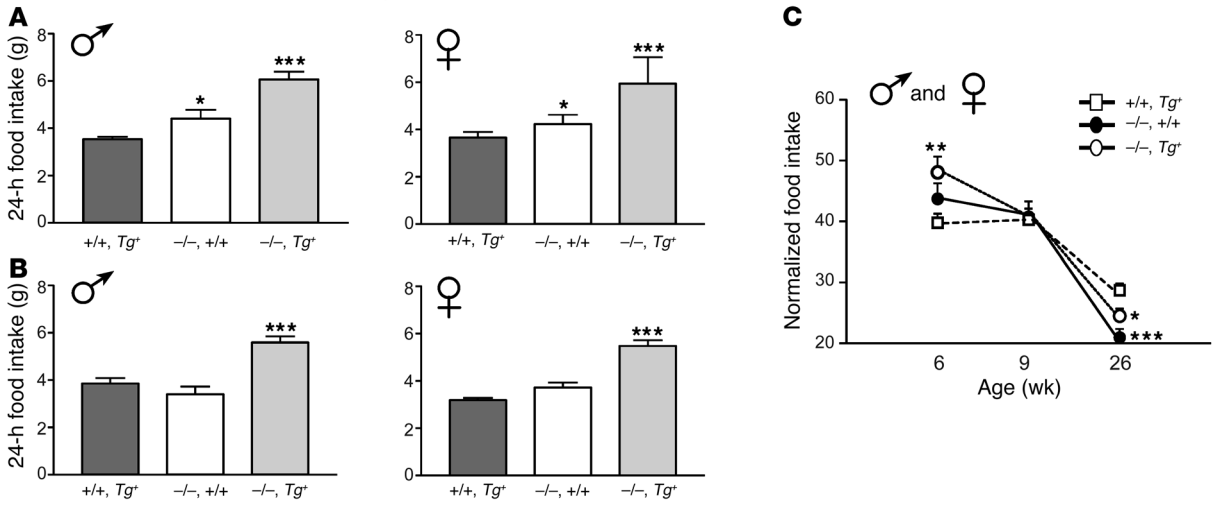

Figure 4
Food intake in *Pomc*$^{+/+}$*Tg*$^{+}$, *Pomc*$^{-/-}$, and *Pomc*$^{-/-}$*Tg*$^{+}$ mice provided ad libitum access to chow. (**A** and **B**) There were genotype differences in 24-hour food intake in 6-week-old males ($F_{2,17} = 25.8$, $P < 0.0001$) and females ($F_{2,15} = 5.418$, $P < 0.05$) (**A**) and in 26-week-old males ($F_{2,19} = 20.2$, $P < 0.0001$) and females ($F_{2,21} = 30.5$, $P < 0.0001$) (**B**). (**C**) Genotype differences were also observed in 24-hour food intake corrected for metabolic mass ([food intake (g)]/[body weight (g)]$^{0.75}$ × 100) at ages 6 weeks ($F_{2,32} = 4.1$, $P < 0.05$) and 26 weeks ($F_{2,45} = 6.6$, $P < 0.005$) but not at age 9 weeks ($F_{2,21} = 0.2$, $P = 0.82$) (males and females combined). *$P < 0.05$, **$P < 0.01$, and ***$P < 0.001$ compared with *Pomc*$^{+/+}$*Tg*$^{+}$.

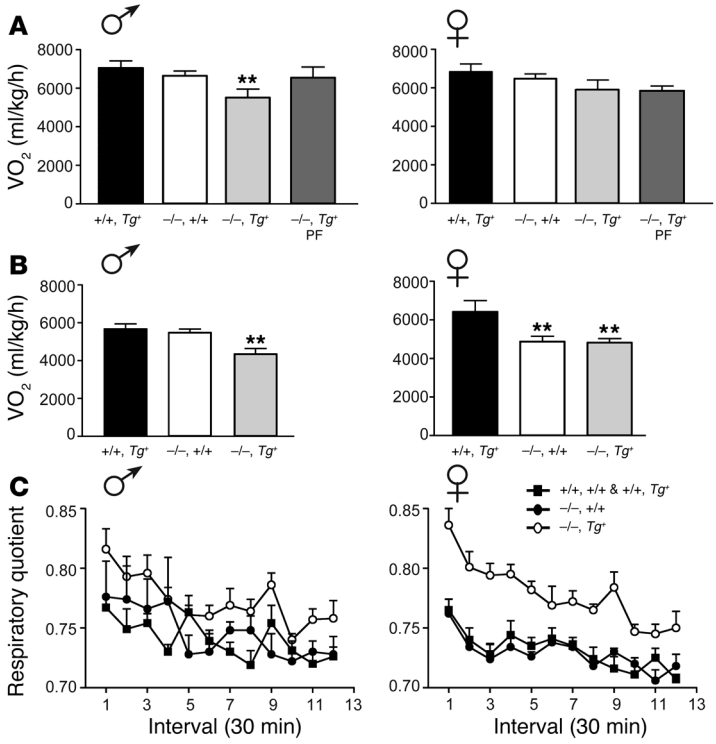

Figure 5

Basal metabolic rate and RQ. (**A** and **B**) Basal metabolic rate measured by VO_2 consumption corrected for metabolic mass (ml/kg$^{0.75}$/h) in 10-week-old (**A**) and 30-week-old (**B**) mice (n = 5–9). Basal metabolic rate differed by genotype in males ($F_{3,18}$ = 3.2, P < 0.05) but not females ($F_{3,20}$ = 1.7, P = 0.19) at age 10 weeks (**A**) and in both males ($F_{2,18}$ = 6.1, P < 0.01) and females ($F_{2,18}$ = 6.8, P < 0.01) at age 30 weeks (**B**). PF, pair-fed. **P < 0.01 compared with *Pomc*$^{+/+}$*Tg*$^{+}$. (**C**) RQ was higher in both male and female *Pomc*$^{-/-}$*Tg*$^{+}$ compared with *Pomc*$^{-/-}$ and *Pomc*$^{+/+}$*Tg*$^{+}$ mice at age 30 weeks. Repeated-measures ANOVAs showed a main effect of genotype for males ($F_{2,198}$ = 3.4, P = 0.05) and females ($F_{2,198}$ = 24.6, P < 0.0001).

genotypes compared with older ages, but the velocity of weight gain was at its maximal slope, VO_2 was trending downward by 5–6% in *Pomc*$^{-/-}$ mice versus *Pomc*$^{+/+}$*Tg*$^{+}$ control mice of both sexes (Figure 5A). However, at age 30 weeks, when the obesity phenotype was fully developed and the velocity of weight gain much more shallow, VO_2 was significantly decreased by 24% in *Pomc*$^{-/-}$ females compared with *Pomc*$^{+/+}$*Tg*$^{+}$ siblings, indicating that the metabolic defect worsened with age and/or degree of obesity (Figure 5B). VO_2 was more consistently altered in *Pomc*$^{-/-}$*Tg*$^{+}$ mice at both ages, with 22% and 15% reductions in males and females, respectively, at 10 weeks and 23% and 27% reductions in males and females, respectively, at 30 weeks compared with control *Pomc*$^{+/+}$*Tg*$^{+}$ mice (Figure 5, A and B).

Furthermore, both sexes of *Pomc*$^{-/-}$*Tg*$^{+}$ mice exhibited elevated respiratory quotients (RQs) at age 30 weeks compared with the other genotypes (Figure 5C). Higher RQs indicate less fatty acid relative to carbohydrate oxidation and possible shifts in energy partitioning and utilization of different energy stores (38).

Caloric restriction attenuated the obesity syndrome in Pomc$^{-/-}$*Tg*$^{+}$ *mice.* To determine whether hyperphagia or decreased metabolic rate was the primary defect in *Pomc*$^{-/-}$*Tg*$^{+}$ mice leading to their massive obesity, we performed a pair-feeding experiment from the earliest possible age (5–6 weeks old) before obesity fully developed and continued until the velocity of weight gain started to decline (15–20 weeks old). Food restriction of *Pomc*$^{-/-}$*Tg*$^{+}$ mice to the average daily intake of *Pomc*$^{+/+}$*Tg*$^{+}$ controls immediately decreased the velocity of weight gain from approximately 2.5 to 0.5 g/wk, identical to that in *Pomc*$^{+/+}$*Tg*$^{+}$ mice provided ad libitum chow (Figure 6A). However, the absolute weight of pair-fed *Pomc*$^{-/-}$*Tg*$^{+}$ mice remained significantly elevated compared with that of *Pomc*$^{+/+}$*Tg*$^{+}$ mice at all time points (P < 0.0001) and was nearly identical to that of ad libitum–fed *Pomc*$^{-/-}$ mice. At age 10 weeks, after 4 weeks of pair-feeding, *Pomc*$^{-/-}$*Tg*$^{+}$ males but not females exhibited an increase in VO_2 to nearly normal levels (Figure 5A).

Consistent with the failure of 10 weeks of caloric restriction to normalize body weight, white fat mass of the pair-fed *Pomc*$^{-/-}$*Tg*$^{+}$ mice was intermediate to that of ad libitum–fed *Pomc*$^{-/-}$*Tg*$^{+}$ and *Pomc*$^{+/+}$*Tg*$^{+}$ mice but similar to that of ad libitum–fed *Pomc*$^{-/-}$ mice for both sexes (Figure 6B). These differences in fat pad weight among genotypes and in response to pair-feeding were mirrored by the concentrations of plasma leptin. Fasting leptin levels were elevated 10-fold in *Pomc*$^{-/-}$*Tg*$^{+}$ mice compared with both *Pomc*$^{-/-}$ and *Pomc*$^{+/+}$*Tg*$^{+}$ mice as early as age 6 weeks (data not shown). Hyperleptinemia became more pronounced at age 9 weeks (Figure 6C), and by age 15–20 weeks, leptin levels were 25-fold higher in ad libitum–fed *Pomc*$^{-/-}$*Tg*$^{+}$ mice compared with *Pomc*$^{+/+}$*Tg*$^{+}$ mice (Figure 6D). In contrast, average leptin levels in ad libitum–fed *Pomc*$^{-/-}$ mice were only 4-fold higher than those in *Pomc*$^{+/+}$*Tg*$^{+}$ controls at age 15–20 weeks (Figure 6D) and also at age 26–30 weeks (data not shown). Pair-feeding of *Pomc*$^{-/-}$*Tg*$^{+}$ mice resulted in substantial reductions in plasma leptin at ages 9 and 15–20 weeks compared with ad libitum feeding, but parallel to the relative changes in fat pad weight, leptin levels of pair-fed *Pomc*$^{-/-}$*Tg*$^{+}$ mice remained higher than those of *Pomc*$^{-/-}$ mice of comparable total body weight.

Corticosterone replacement augmented weight gain and obesity in Pomc$^{-/-}$ *mice.* To determine whether glucocorticoids, independently of pituitary POMC, accounted for the increased obesity phenotype in the genetically rescued mice, we performed 2 pharmacological replacement experiments, treating *Pomc*$^{-/-}$ mice of both sexes with a fixed concentration of 25 μg corticosterone per milliliter drinking water.

In the first experiment, groups of male and female *Pomc*$^{-/-}$ mice were chronically treated with corticosterone in their drinking water starting at age 5–6 weeks or provided with ordinary drinking water. Diurnal corticosterone levels in the treated *Pomc*$^{-/-}$ mice at ages 10–15 weeks were within the physiological range: 0800 hours male, 41 ± 16 ng/ml; 0800 hours female, 26 ± 1 ng/ml; 2000 hours male, 70 ± 45 ng/ml; 2000 hours female, 76 ± 51 ng/ml. Corticosterone-replaced *Pomc*$^{-/-}$ mice (n = 8) gained significantly more weight over 9 weeks than the untreated *Pomc*$^{-/-}$ mice (n = 11): males, 20.3 ± 0.6 g versus 8.4 ± 1.9 g (P < 0.005, Student's t test); females, 13.2 ± 0.9 g versus 6.1 ± 1.1 g (P < 0.001, Student's t test). Corticosterone replacement also resulted in significantly greater white fat pad mass (males, 8.1 ± 0.3 g versus 2.3 ± 0.7 g, P = 0.002; females, 6.9 ± 0.8 g versus 4.1 ± 0.6 g, P = 0.02, Student's t test) and plasma leptin levels (males, 73 ± 11 ng/ml versus 12 ± 7 ng/ml, P < 0.01; females, 68 ± 12 ng/ml versus 14 ± 4 ng/ml, P = 0.01, Student's t test) at 17–20 weeks of age compared with no treatment.

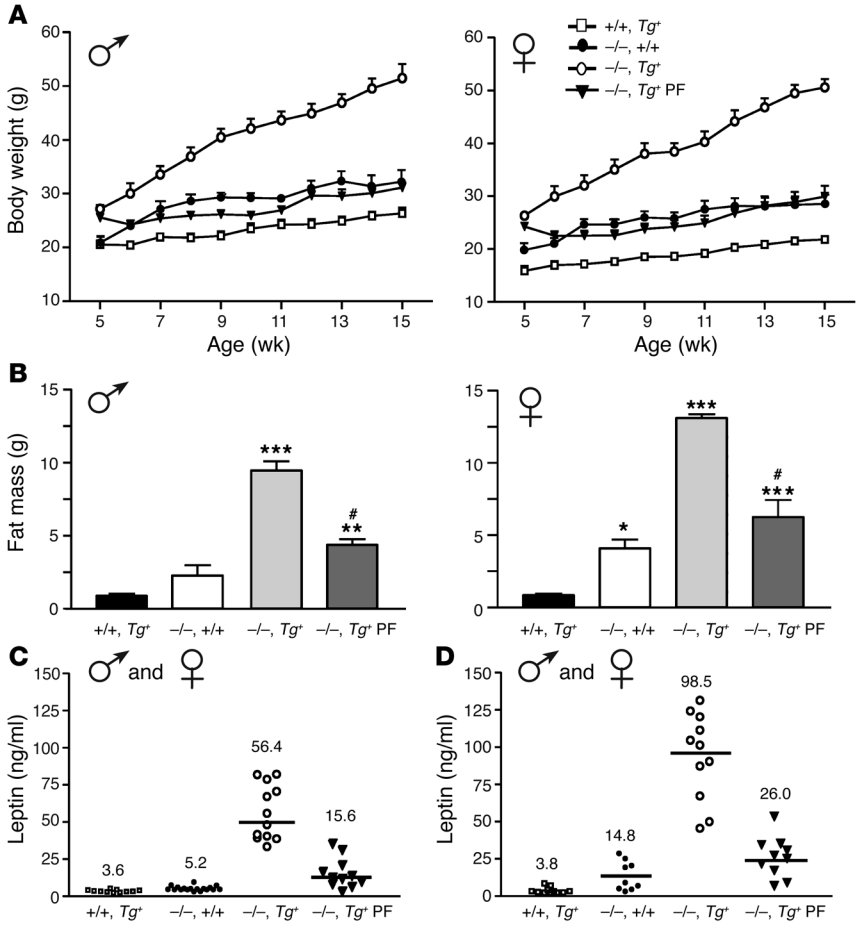

Figure 6
Growth curves, fat mass, and plasma leptin levels of individually housed *Pomc*$^{+/+}$*Tg*$^{+}$, *Pomc*$^{-/-}$, and *Pomc*$^{-/-}$*Tg*$^{+}$ mice from ages 5 to 15 weeks. (**A**) The effect on body weight of pair-feeding (PF) of *Pomc*$^{-/-}$*Tg*$^{+}$ mice to the daily food intake of *Pomc*$^{+/+}$*Tg*$^{+}$ mice starting at age 5 weeks (n = 5–11). Repeated-measures ANOVAs over the 10-week period showed a main effect of group for males ($F_{18,117}$ = 21.5, P < 0.0001) and females ($F_{18,144}$ = 24.6, P < 0.0001). One-factor ANOVAs showed that *Pomc*$^{-/-}$*Tg*$^{+}$ pair-fed mice differed from *Pomc*$^{-/-}$*Tg*$^{+}$ mice fed ad libitum and *Pomc*$^{+/+}$*Tg*$^{+}$ mice fed ad libitum (P < 0.001); *Pomc*$^{-/-}$ mice fed ad libitum also differed from *Pomc*$^{+/+}$*Tg*$^{+}$ mice fed ad libitum and *Pomc*$^{-/-}$*Tg*$^{+}$ mice fed ad libitum (P < 0.001) but not from *Pomc*$^{-/-}$*Tg*$^{+}$ pair-fed mice. (**B**) The effects of pair-feeding of *Pomc*$^{-/-}$*Tg*$^{+}$ mice on accumulation of fat mass. The combined weight of 4 white fat pads (renal, visceral, gonadal, and inguinal) was different among groups in 15- to 20-week-old male ($F_{3,17}$ = 50.3, P < 0.0001) and female ($F_{3,23}$=35.9, P<0.0001) mice. *P<0.05, **P<0.001, and ***P < 0.0001 compared with *Pomc*$^{+/+}$*Tg*$^{+}$; $^{\#}P$ < 0.0001 compared with *Pomc*$^{-/-}$*Tg*$^{+}$. (**C** and **D**) The effect of pair-feeding of *Pomc*$^{-/-}$*Tg*$^{+}$ mice on plasma leptin levels. Data are the means and scattergrams of all individual leptin levels (n = 9–19) obtained after a 16-hour overnight fast in 9-week-old (**C**) and ad libitum–fed 15- to 20-week-old (**D**) mice of both sexes.

Using a within-subjects design, a second group of 6- to 9-week-old *Pomc*$^{-/-}$ mice was treated sequentially with corticosterone for 16 days, ordinary drinking water for 9 days, and corticosterone for a final 9 days. The velocity of weight gain during each corticosterone replacement period was approximately 4 g/wk, while all mice lost weight at a rate of approximately 2 g/wk when switched from corticosterone to water (Figure 7A, top). Separate groups of age-matched WT C57BL/6J *Pomc*$^{+/+}$ mice were treated with either corticosterone or ordinary drinking water continuously for the entire 5-week study and had indistinguishable growth curves with a velocity of weight gain of approximately 0.4 g/wk, regardless of treatment or sex (Figure 7A, bottom). Corticosterone treatment significantly increased daily food intake by more than 50% in all the *Pomc*$^{-/-}$ mice but had no effect in *Pomc*$^{+/+}$ mice of either sex (Figure 7B).

Corticosterone supplementation in the drinking water resulted in different plasma hormone levels between male and female mice for both genotypes (Figure 7C), despite the absence of sex differences in weight gain and food intake for either genotype. Untreated *Pomc*$^{+/+}$ mice exhibited a normal circadian variation in plasma corticosterone with lower levels at 0800 hours and higher levels at 2400 hours and sexual dimorphism with higher levels at both time points in females. Corticosterone supplementation had little effect on this pattern in *Pomc*$^{+/+}$ females and failed to increase plasma levels above the sensitivity of the RIA (12.5 ng/ml) in the 2 *Pomc*$^{-/-}$ female mice at either time point. While most untreated *Pomc*$^{+/+}$ males also had undetectable plasma corticosterone levels at 0800 hours, corticosterone replacement significantly increased plasma levels of the steroid hormone at both time points in *Pomc*$^{+/+}$ and *Pomc*$^{-/-}$ male mice, and to a similar magnitude.

Discussion

We generated and analyzed a novel strain of compound mutant mice with a de facto neuron-specific deficiency of POMC. The principal finding was that the syndrome of obesity associated with hyperphagia and metabolic disturbances characterized originally by Yaswen et al. (7) and independently by Challis et al. (39) was markedly accentuated in mice with the selective restoration of peripheral POMC compared with mice with a global absence of POMC peptides.

The phenotype of *Pomc*$^{-/-}$*Tg*$^{+}$ mice was characterized by marked increases in white adipose tissue with a disproportionately greater increase in subcutaneous fat, massive hepatomegaly with steatosis, and extreme insulin resistance and hyperleptinemia. In contrast, *Pomc*$^{-/-}$ mice attained a final body mass intermediate to WT and *Pomc*$^{-/-}$*Tg*$^{+}$ mice and accumulated excess fat principally in their gonadal depots, a subset of intra-abdominal fat whose mass is typically directly proportional to insulin resistance in humans and mice (40, 41) whereas subcutaneous fat deposition correlates better with increased circulating leptin (2, 41). *Pomc*$^{+/-}$ mice also exhibited a mild obesity syndrome, similar to the intermediate phenotype observed by Coll et al. (42) in their 129 strain *Pomc*$^{+/-}$ mice fed a high-fat diet. The predominantly C57BL/6J

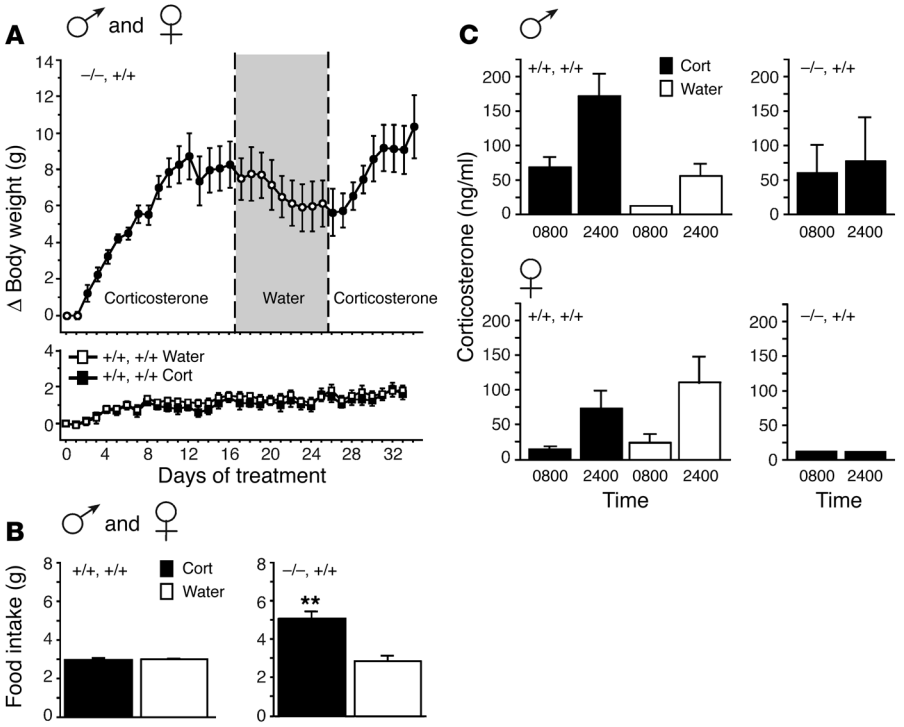

Figure 7

The effect on body weight, food intake, and plasma corticosterone levels of corticosterone (Cort) replacement (25 μg/ml drinking water) in *Pomc*$^{-/-}$ and C57BL/6J *Pomc*$^{+/+}$ mice starting at age 6–9 weeks. *Pomc*$^{+/+}$ mice (n = 20; 10 males and 10 females) were separated into 2 groups and received either water (n = 10) or corticosterone (n = 10) for 34 consecutive days. All *Pomc*$^{-/-}$ mice (n = 5; 3 males and 2 females) were first given corticosterone (days 1–16, filled circles), then water (days 16–25, open circles), and finally corticosterone again (days 25–34, filled circles). (**A**) Weight gain was significantly accelerated by corticosterone replacement in *Pomc*$^{-/-}$ mice but was unaltered in *Pomc*$^{+/+}$ mice of either sex. (**B**) Average daily food intake measured over a 7-day period was increased in *Pomc*$^{-/-}$ mice (corticosterone versus water, $^{**}P = 0.01$, paired t test) but was unchanged by corticosterone treatment in *Pomc*$^{+/+}$ mice. (**C**) Plasma corticosterone levels obtained under stress-free conditions at 0800 and 2400 hours. Corticosterone was always less than 12.5 ng/ml (assay sensitivity) for *Pomc*$^{-/-}$ mice without replacement (data not shown).

genetic background of mice in our studies likely accounts for the increased obesity susceptibility of *Pomc*$^{+/-}$ animals on low-fat chow. Comparisons of young and middle-aged animals showed that excess storage of white fat occurred earlier in *Pomc*$^{-/-}$*Tg*$^{+}$ than in *Pomc*$^{-/-}$ mice. In parallel, plasma leptin levels were already 10-fold elevated in 6-week-old *Pomc*$^{-/-}$*Tg*$^{+}$ mice compared with WT controls, while *Pomc*$^{-/-}$ mice had essentially normal leptin levels, reflecting their delayed accumulation of excess fat.

Males and females of each mutant genotype generally exhibited parallel changes in the measured biochemical, physiological, and behavioral parameters that assessed energy balance. The magnitude of change for many variables, however, was often influenced by sex. Notably, the greatest percentage increase in total body mass and subcutaneous fat relative to WT controls occurred in female *Pomc*$^{-/-}$*Tg*$^{+}$ mice, even though they exhibited only minimal dysregulation of their HPA axis relative to *Pomc*$^{-/-}$*Tg*$^{+}$ males. Conversely, the phenotypic effects of *Pomc*$^{+/-}$ mutations were largely evident only in males. These sexual dimorphisms in the mutant mice are most likely a result of sex steroid interactions on multiple pathways known to affect energy homeostasis (43–45).

Hyperphagia and decreased energy expenditure contribute to the obesity phenotype of Pomc mutant mice. The initial characterization of 2 independent lines of *Pomc*$^{-/-}$ mutant mice by Yaswen et al. (7) and later by Challis et al. (39) suggested that both hyperphagia and decreased metabolic rate contributed to the obesity phenotype. We therefore used pair-feeding experiments to test whether hyperphagia and/or metabolic defects were primarily responsible for the increased body weight in *Pomc*$^{-/-}$*Tg*$^{+}$ mice. If a metabolic defect exists independently of hyperphagia, the mice would be predicted to still develop obesity when food-restricted. *Pomc*$^{-/-}$*Tg*$^{+}$ mutant mice slightly reduced their body weight during the first week of pair-feeding. However, after prolonged caloric restriction, the absolute body weight of *Pomc*$^{-/-}$*Tg*$^{+}$ mice rebounded, and their growth velocity remained roughly parallel to that of freely feeding *Pomc*$^{+/+}$*Tg*$^{+}$ mice. Furthermore, leptin levels remained elevated and the pair-fed mice continued to accumulate fat mass, supporting a combination of disturbances in metabolism and appetite. An unavoidable caveat for the pair-feeding experiment is that body weight of the *Pomc*$^{-/-}$*Tg*$^{+}$ mice was already significantly greater than that of control *Pomc*$^{+/+}$*Tg*$^{+}$ mice at the start. Attempts to individually house mice immediately after weaning when the weight differences were minimal led to a failure to thrive in many instances, resulting in a compromise of age 4–5 weeks for initiation of pair-feeding with individually housed mice.

In our study, hyperphagia was evident early in both *Pomc*$^{-/-}$*Tg*$^{+}$ and *Pomc*$^{-/-}$ mice whether food intake was expressed in absolute values or normalized to total estimated metabolic mass (37). However, in the following weeks, absolute food consumption was not modified, despite a sustained increase in body weight. Consequently the rank order for feed efficiency (ratio of weight gain to caloric intake) between ages 6 and 9 weeks among genotypes was *Pomc*$^{-/-}$*Tg*$^{+}$ > *Pomc*$^{-/-}$ > *Pomc*$^{+/+}$*Tg*$^{+}$, indicating a predominant partitioning of fuel stores into fat in *Pomc*$^{-/-}$*Tg*$^{+}$ mice and *Pomc*$^{-/-}$ mice. This trend of increased feed efficiency was even more pronounced in older animals, especially in adult 26-week-old *Pomc*$^{-/-}$ mice, whose absolute daily food intake was indistinguishable from that of age- and sex-matched *Pomc*$^{+/+}$ mice. After correction for metabolic mass, both *Pomc*$^{-/-}$ and *Pomc*$^{-/-}$*Tg*$^{+}$ mice appeared to be hypophagic compared with their WT siblings at 26 weeks. If we assume that caloric intake must be increased proportionately to body mass to maintain body weight gain, hyperphagia cannot fully explain the maintenance of obesity in adult animals.

Our data differ from those obtained in a pair-feeding study of MC4-R KO mice (20), where a metabolic defect was suggested to be the primary mechanism for obesity, accompanied by second-

ary hyperphagia to support the animals' increased body weight. However, another set of experiments comparing younger (3- to 5-week-old) and adult MC4-R KO mice indicated that the earliest onset of excessive fat accumulation was a result of primary hyperphagia partially counteracted by increased metabolic rate (46). The physiological mechanisms supporting obesity in either *Pomc*$^{-/-}$ or *Pomc*$^{-/-}$*Tg*$^{+}$ mice would not necessarily be expected to be identical to those in MC4-R KO mice, because of the additional role of MC3-R in maintaining energy homeostasis. MC3-R KO mice have a unique phenotype characterized by increased fat mass and decreased lean body mass, hypophagia with increased feed efficiency, and unusual metabolic changes (23, 24). Indeed, the growth and obesity phenotype of the *Pomc*$^{-/-}$*Tg*$^{+}$ mice is apparently most similar to that of the combined MC4-R and MC3-R double-KO mice, which exhibit an additive phenotype for absolute increase in body mass compared with either of the single-receptor-KO mice (24). Conclusions from each of these previous studies, as well as from our own experiments, on the primacy of hyperphagia versus decreased metabolism must be tempered by the recognized difficulties inherent in the quantitation of energy expenditure and comparison between animals that differ greatly in body mass and composition.

Peripheral and central actions of glucocorticoids combine to augment the obesity phenotype in Pomc$^{-/-}$*Tg*$^{+}$ *versus Pomc*$^{-/-}$ *mice*. Glucocorticoids might function peripherally to produce the observed genotype differences in the onset of fat accumulation and elevation of plasma leptin, not only by favoring leptin production (47, 48), but also by inducing a repartition of lipid storage among specific fat pads including subcutaneous fat and the liver, where gluconeogenesis is stimulated by corticosterone. Intra-abdominal fat is known to exhibit an increased lipolytic response via the stimulation of adrenergic receptors (49). Because *Pomc*$^{-/-}$ mice lack secretion of epinephrine in addition to corticosterone from their atrophic adrenals (7), reduced lipolysis in gonadal fat could lead to increased storage in this site relative to subcutaneous adipocytes and explain partitioning differences.

Adipose tissue produces leptin in conditions of positive energy balance (50), thereby contributing to reduced caloric intake, increased metabolism, and a net restoration of energy homeostasis. However, *Pomc*$^{-/-}$*Tg*$^{+}$ mice displayed hyperphagia and decreased metabolic rate despite elevated leptin levels. Although leptin directly stimulates POMC neurons (6), recent data have demonstrated that the effects of exogenous leptin administration on food intake and body weight were intact in 4-week-old nonobese *Pomc*$^{-/-}$ mice and attenuated in 12- to 15-week-old obese *Pomc*$^{-/-}$ mice, suggesting that leptin resistance develops concordantly with the increasing weight by a POMC-independent pathway (39). Glucocorticoids likely contribute to the apparently greater leptin resistance in *Pomc*$^{-/-}$*Tg*$^{+}$ mice and explain their reduced metabolism and increased body weight compared with *Pomc*$^{-/-}$ mice. Indeed, glucocorticoids play an inhibitory role in leptin actions. Leptin has more potent and long-lasting effects to decrease body weight and food intake when administered to adrenalectomized rats (51, 52). Furthermore, glucocorticoids can attenuate the effects of centrally administered leptin on feeding and metabolism (51).

Glucocorticoids also exhibit a permissive role in the development of obesity that is independent of leptin, but associated with hyperinsulinemia and insulin resistance. In genetic models of obesity, such as *ob/ob* mice and *fa/fa* rats, withdrawal of glucocorticoids by adrenalectomy either prevents or ameliorates several defects associated with obesity (increased food intake, increased body weight, increased fat storage, high plasma glucose and insulin levels), and these effects can be reversed by glucocorticoid replacement (28, 32, 53, 54). Some of these responses may be attributed to a sensitizing effect of glucocorticoid withdrawal on the anorectic action of MC4-R activation (52). However, similar reductions of circulating corticosterone by adrenalectomy do not attenuate diet-induced obesity in WT C57BL/6 mice (55).

Additional studies have suggested that the observed anabolic effects of glucocorticoids are mediated in part at the level of the CNS. Smaller doses of glucocorticoids are more efficient at inducing obesity after injection directly into the brain than after injection into the periphery (56–58), and this difference is presumably mediated by central glucocorticoid receptors. In support of this central role, selective inactivation of glucocorticoid receptors in the CNS affects energy accumulation by reducing food intake and growth of lean body mass, but increasing fat accumulation (59).

Our data as well as the literature support the hypothesis that the severe metabolic syndrome of *Pomc*$^{-/-}$*Tg*$^{+}$ mice results from permissive actions of glucocorticoids in combination with a central loss of POMC signaling rather than the simpler alternative of direct effects of hypercorticosteronemia. Indeed, although male *Pomc*$^{-/-}$*Tg*$^{+}$ mice exhibited clearly elevated corticosterone levels, the greater percentage increase in body weight in *Pomc*$^{-/-}$*Tg*$^{+}$ than in *Pomc*$^{-/-}$ mice occurred in females. Interestingly, the adipose tissue with the disproportionately greatest increase in mass in the *Pomc*$^{-/-}$*Tg*$^{+}$ mice was subcutaneous inguinal fat and not visceral fat as might be predicted from hypercorticosteronemia. Mice with central overexpression of corticotropin-releasing hormone and a similar pattern of chronic hypercorticosteronemia to that of *Pomc*$^{-/-}$*Tg*$^{+}$ mice do not gain excessive total weight and in fact have reduced body weight, although with anecdotally reported truncal obesity (60). We have also found that male somatostatin-deficient mice exhibit a very similar pattern of enlarged adrenal glands and elevated peak diurnal corticosterone levels comparable to that in male *Pomc*$^{-/-}$*Tg*$^{+}$ mice but do not develop the obesity syndrome (ref. 61 and our unpublished data). Finally, many other genetic models of obesity in rats and mice (*fa/fa*, *ob/ob*, *db/db*, and *Ay/a*) exhibit elevated circulating corticosterone levels or increased tissue corticosterone, although excessive glucocorticoid tone is not considered to be the primary mechanism for obesity (62).

Therefore, to further analyze the contribution of glucocorticoids with a concomitant absence of central and peripheral POMC to energy balance, we treated *Pomc*$^{-/-}$ mice with corticosterone in their drinking water. Acute treatment induced an immediate increase in the rate of body weight gain and food consumption in *Pomc*$^{-/-}$ mice. These effects were rapidly reversed with treatment interruption and restored after the animals were again treated with corticosterone. Continuous replacement for several weeks was accompanied by accumulation of fat mass and hyperleptinemia, nearly comparable to the genetic rescue of pituitary POMC production, in both male and female *Pomc*$^{-/-}$ mice. In contrast, the identical corticosterone supplementation of drinking water did not alter weight gain or food intake in WT male or female C57BL/6J mice, consistent with previously published results (63). These data clearly suggest a permissive or synergistic action of glucocorticoids in *Pomc*$^{-/-}$ mice. A recent study using an identical method of corticosterone replacement in a different strain of *Pomc*$^{-/-}$ mice on a 129 genetic background reported similar metabolic consequences but with greater adverse effects on the animals' overall health (64).

In a dynamic homeostatic system, the interaction of glucocorticoids with numerous factors to exert its overall effects on energy balance is complicated by the impossibility of keeping only 1 important physiological factor constant without changing others. The effects of corticosterone have to be considered together with the absence or presence of POMC peptides, either globally or specifically from the brain. Thus, a contribution of peripheral melanocortin peptides to the obesity phenotype independently of glucocorticoid secretion cannot totally be excluded from our study, since the phenotype of *Pomc*$^{-/-}$*Tg*$^{+}$ mice in the absence of circulating corticosterone has not been evaluated. Peripheral administration of αMSH agonists has been shown to cause weight loss in mice with high-fat diet–induced obesity and genetically obese mice (65–67), and in *fa/fa* rats (68, 69). In addition, systemic injection of [Nle^4, D-Phe^7]-melanocyte-stimulating hormone reduced food intake and weight gain in *Pomc*$^{-/-}$ mice (7). Although potent and degradation-resistant MSH analogs have been suggested to exert much of their effect within the CNS after peripheral administration (12), other studies indicate that systemically administered MTII crossed the blood-brain barrier poorly (70) and may also act on peripheral systems.

In conclusion, the present study confirms and extends previous reports that *Pomc*$^{-/-}$ mice develop obesity with modest hyperphagia and decreased metabolic rate despite the absence of circulating glucocorticoids (7, 39). This phenotype was not averted by restoration of physiological levels of pituitary POMC peptides including αMSH but instead was exacerbated by a combination of severe hyperphagia and increased feed efficiency. Corticosterone treatment of *Pomc*$^{-/-}$ mice recapitulated the phenotype, indicating that a permissive action of glucocorticoids together with the CNS deficiency of POMC accounts for the morbid obesity in genetically altered *Pomc*$^{-/-}$*Tg*$^{+}$ mice. A potential contribution of peripheral POMC peptides to the phenotype may have been masked by the metabolic effect of glucocorticoids and could be further explored in future experiments by clamping of corticosterone in rescued mice or creation of a de facto lack of peripheral POMC. Finally, the sustained hyperphagia, velocity of weight gain, and eventual peaks of total body and fat mass achieved in *Pomc*$^{-/-}$*Tg*$^{+}$ mice despite a diet containing only 5% fat-derived calories are all significantly greater than those reported previously for any of the single-gene MC4-R, MC3-R, or β-endorphin KO mouse strains (19, 23–25). Indeed, the extreme obesity phenotype of *Pomc*$^{-/-}$*Tg*$^{+}$ mice strongly supports the contention made previously by Chen et al. (24), based on their genetic cross of MC4-R and MC3-R KOs to produce a double-KO strain, that the 2 melanocortin receptor subtypes play critical and distinct roles in the CNS regulation of energy balance by POMC-derived peptides.

Methods

Transgene construction. A 9.7-kb *EcoRI-EcoRI* mouse genomic DNA fragment containing the 3 *Pomc* exons and proximal promoter elements (35) was subcloned into pBluescript SK (Stratagene) and used to construct the pituitary-specific POMC rescue transgene *pHalEx2**. A pair of complementary 23-bp oligonucleotides (5′-CCCGGGCTCGAGTTTAAAGCGCG-3′ and 5′-CGCGCTTTAAACTCGAGCCCGGG-3′) was annealed to form a blunt-ended double-stranded DNA fragment and ligated into a *StuI* site in the 5′ untranslated region of exon 2. The correctly inserted oligonucleotide was designed for specific detection of *pHalEx2** mRNA without altering translation or processing of POMC.

Generation and breeding of mice. A colony of *Pomc* mutant mice on a B6;129X1;129S6 hybrid genetic background was established as described previously (71). The novel strain of transgenic mice was generated by nuclear microinjection of linearized *pHalEx2* Tg* DNA into B6D2 F_2 hybrid 1-cell embryos using standard techniques. The *pHalEx2* Tg* allele was backcrossed from a single identified founder to inbred C57BL/6J mice (Jackson Laboratory) for 2 consecutive generations and subsequently crossed onto the *Pomc*$^{-/-}$ genetic background by an additional 2 generations of double-heterozygous matings. Consequently, the resulting hybrid genetic background of the compound mutant and sibling control mice was approximately 80% C57BL/6, 10% DBA/2, and 10% 129X1;129S6. Mice were maintained under controlled temperature and photoperiod (12 hours light, 12 hours dark; lights on at 0700 hours) with free access to water and a standard rodent chow (5% fat, 19% protein, 5% fiber, 3.4 kcal/g), except where noted. All experimental protocols were approved by the Oregon Health & University Institutional Animal Care and Use Committee and followed Public Health Service guidelines.

Genotyping. Three separate PCR reactions were used to identify the *Pomc* alleles from genomic DNA samples. Touchdown PCR conditions were: 15 cycles at 94°C for 30 seconds, 64°C minus 1°C per cycle for 30 seconds, and 72°C for 30 seconds; 15 cycles of 94°C for 30 seconds, 50°C for 30 seconds, and 72°C for 30 seconds; and 72°C for 3 minutes. The primer pairs and sizes of specific amplified bands were: *Pomc*$^{+}$ 318-bp product, primer pair i 5′-GCTTGCATCCGGGCTTGCAAACT-3′ and ii 5′-AGCAACGTTGGGGTACACCTTC-3′; *Pomc*$^{-}$ approximately 300-bp product, primer pair iii 5′-TTGTTAACTTGTTTATTGCAGCTT-3′ and iv 5′-ATGAGAAATTGGGCCATGGGACTGAC-3′; and *pHalEx2* Tg* 226-bp product, primer pair v 5′-TAGTGTTGGCTCAATGTCCT-3′ and vi 5′-GCTCTCCAGGCACCAGCTCC-3′.

Analysis of POMC peptide expression. Mice were anesthetized with 2% Avertin, perfused via the left ventricle with 4% buffered paraformaldehyde, and their brains and pituitary glands were removed and postfixed for 16 hours. Immunohistochemistry was performed on 12-μm frozen pituitary sections (after equilibration in 20% sucrose) and free-floating 50-μm vibratome sections incubated with 2% normal goat serum and 0.3% Triton X-100 in 10 mM potassium phosphate–buffered saline containing anti–rat ACTH (1:16,000) or anti–β-endorphin (1:16,000) primary antiserum (both from A. Parlow, National Hormone and Peptide Program, Harbor-UCLA Medical Center, Torrance, California, USA) at 4°C overnight. Sections were then rinsed in potassium phosphate–buffered saline and sequentially incubated with 20 μg/ml biotinylated goat anti-rabbit IgG (Vector Laboratories) for 2 hours at 25°C followed by incubation with an avidin-biotin/HRP complex (VECTASTAIN Elite ABC Kit; Vector Laboratories) for 1 hour at 25°C. Reaction product was revealed with 1 mg/ml diaminobenzidine containing 0.03% H_2O_2, yielding a brown precipitate.

For quantitation of αMSH, individual whole pituitary glands and 15- to 20-mg blocks containing the medial basal hypothalamus were collected from mice into tubes with 0.5 ml 2% acetic acid containing 10 mg/ml BSA. Peptides were extracted by 3 rounds of freeze-thawing and sonication, insoluble material was removed by centrifugation, and supernatants were neutralized with 10 M NaOH. Serial dilutions of the tissue extracts were prepared in assay buffer for RIA according to the manufacturer's instructions (EURIA-α-MSH; Euro-Diagnostica, ALPCO). Stated cross-reactivities of the assay are: αMSH, 100%; des-acetyl-αMSH, 100%; and des-amido-αMSH, ACTH 1-13, ACTH 1-24, ACTH 1-39, βMSH, and γMSH, all less than 0.002%.

General study design. Two cohorts of mice were generated by breeding strategies described above. The first cohort consisted of approximately 250 mice that were housed in groups of 4–6 mixed-genotype first-degree relatives for most of their lifetimes except where indicated. These mice

were provided food ad libitum and weighed weekly from ages 1 to 26 weeks, and then subgroups were killed at subsequent time points for body composition and other analyses. A second younger cohort of approximately 100 mice was generated for pair-feeding and corticosterone replacement experiments.

Pair-feeding experiments and corticosterone replacement. *Pomc*$^{+/+}$*Tg*$^{+}$, *Pomc*$^{-/-}$, and *Pomc*$^{-/-}$*Tg*$^{+}$ mice of both sexes from cohort 2 were individually housed starting at age 4–5 weeks (approximately 1–2 weeks after weaning) until conclusion of the experiments, provided with food ad libitum, and weighed weekly. For pair-feeding experiments, food intake was measured daily, and a subgroup of *Pomc*$^{-/-}$*Tg*$^{+}$ mice were provided the average amount of food that their sex- and age-matched *Pomc*$^{+/+}$*Tg*$^{+}$ controls consumed daily as a single meal at 1800 hours from age 5 weeks to the end of the experiment. To determine the contribution of circulating glucocorticoids in development of the obesity phenotype, other subgroups of body weight–matched *Pomc*$^{-/-}$ mice were treated with corticosterone (25 μg/ml) in their drinking water either continuously or intermittently starting at age 6 weeks. This dose was chosen because previous studies showed that it restored low physiological levels of the hormone in adrenalectomized male mice. At 15–20 weeks old, mice were killed and fat pads weighed. Groups of C57BL/6J male and female mice were supplemented with the same dose of corticosterone from ages 6 to 11 weeks to determine the effects on body weight and food intake in WT animals.

Food consumption, basal metabolic rate, and RQ. In 6- and 9-week-old mice individually housed from age 5 weeks, food consumption was determined over a 24-hour period. Twenty-six-week-old mice that had been group-housed were habituated to individual housing for 9 days to restabilize feeding behavior after the initial period of stress-induced anorexia, and then their average 24-hour food intake was calculated over 5 consecutive measurements on days 10–14. In addition to the raw data, daily food intake was normalized to metabolic mass using the following scaling formula: [food intake (g)]/[body weight (g)]$^{0.75}$ × 100 (37). Twenty-four-hour food intake in the corticosterone replacement studies was calculated over 7 consecutive daily measurements for each mouse.

Basal metabolic rate was assessed in 10- and 30-week-old mice using an indirect open-circuit calorimeter system (Oxymax; Columbus Instruments) consisting of acrylic chambers with dimensions of 10.5 × 20.5 × 12.5 cm that limited spontaneous locomotor activity. Mice were placed into individual chambers at 0800 hours for 6 hours without access to food or water for 2 consecutive days to allow for habituation. On the third day, a total of 12 measurements were recorded from each mouse at 30-minute intervals. The inlet fresh air flow rate was 0.5 l/min with a sample-flow rate of 0.4 l/min. Each chamber was sampled for 50 seconds with a resting time of 150 seconds. Individual basal oxygen consumption (VO_2) levels were established by averaging of the 3 lowest of 12 VO_2 measurements. CO_2 production from each mouse was also recorded simultaneously and used to calculate the RQ (RQ = VCO_2/VO_2) at each 30-minute interval.

Plasma glucose and hormone levels. Blood for glucose, insulin, and leptin measurements was obtained by tail bleeding and collected into heparinized capillary tubes between 0800 and 1000 hours following a 16- or 24-hour fast from mice of the indicated ages or from ad libitum–fed 15- to 20-week-old mice. Samples were centrifuged at 3,000 *g* for 5 minutes, and the plasma was stored frozen at –20°C. The first drop of whole blood was used for glucose determination using a glucometer (Elite XL; Bayer). To measure circadian corticosterone levels, blood was collected from the tail tip of unanesthetized mice at the indicated time points. All samples were collected less than 1 minute after cage disturbance, and only 1 sample was collected per mouse per day. Plasma hormones were measured using a corticosterone RIA (MP Biomedicals Inc.), a rat insulin RIA (Linco Research Inc.), and a mouse-specific leptin RIA (Linco Research Inc.) according to the manufacturers' instructions.

Statistics. All data presented are the mean ± SEM unless otherwise stated and were analyzed by either multifactor ANOVA with sex and genotype as independent variables or repeated-measures ANOVA for body weight curves and RQ, using StatView Power PC version for Macintosh (version 5.0.1; SAS Institute Inc.). Post hoc pairwise comparisons between groups were performed by Fisher's protected least squares difference. Two-tailed Student's *t* test was used for comparisons involving only 2 groups. *P* values less than 0.05 were considered significant.

Acknowledgments

We thank U. Hochgeschwender for supplying the original breeder pair of *Pomc*$^{+/-}$ mice and W. Fan for assistance with the Oxymax system. This work was funded by NIH grants DK66604 (to M.J. Low) and HG00201 (to J.L. Smart). V. Tolle was the recipient of an American Society for Pharmacology and Experimental Therapeutics/Merck postdoctoral fellowship in integrative pharmacology.

Received for publication April 4, 2005, and accepted in revised form November 29, 2005.

Address correspondence to: Malcolm J. Low, Vollum Institute, L474, Oregon Health & Science University, 3181 SW Sam Jackson Park Road, Portland, Oregon 97239, USA. Phone: (503) 494-4672; Fax: (503) 494-4976; E-mail: low@ohsu.edu.

James L. Smart and Virginie Tolle contributed equally to this work.

1. Isomaa, B. 2003. A major health hazard: the metabolic syndrome. *Life Sci.* **73**:2395–2411.
2. Havel, P.J. 2001. Peripheral signals conveying metabolic information to the brain: short-term and long-term regulation of food intake and energy homeostasis. *Exp. Biol. Med.* **226**:963–977.
3. Dallman, M.F., et al. 2003. A spoonful of sugar: feedback signals of energy stores and corticosterone regulate responses to chronic stress. *Physiol. Behav.* **79**:3–12.
4. Low, M.J. 2004. Role of proopiomelanocortin neurons and peptides in the regulation of energy homeostasis. *J. Endocrinol. Invest.* **27**:95–100.
5. Ellacott, K.L., and Cone, R.D. 2004. The central melanocortin system and the integration of short- and long-term regulators of energy homeostasis. *Recent Prog. Horm. Res.* **59**:395–408.
6. Cowley, M.A., et al. 2001. Leptin activates anorexigenic POMC neurons through a neural network in the arcuate nucleus. *Nature.* **411**:480–484.
7. Yaswen, L., Diehl, N., Brennan, M.B., and Hochgeschwender, U. 1999. Obesity in the mouse model of pro-opiomelanocortin deficiency responds to peripheral melanocortin. *Nat. Med.* **5**:1066–1070.
8. Krude, H., et al. 1998. Severe early-onset obesity, adrenal insufficiency and red hair pigmentation caused by POMC mutations in humans. *Nat. Genet.* **19**:155–157.
9. Challis, B.G., et al. 2002. A missense mutation disrupting a dibasic prohormone processing site in pro-opiomelanocortin (POMC) increases susceptibility to early-onset obesity through a novel molecular mechanism. *Hum. Mol. Genet.* **11**:1997–2004.
10. McMinn, J.E., Wilkinson, C.W., Havel, P.J., Woods, S.C., and Schwartz, M.W. 2000. Effect of intracerebroventricular alpha-MSH on food intake, adiposity, c-Fos induction, and neuropeptide expression. *Am. J. Physiol. Regul. Integr. Comp. Physiol.* **279**:R695–R703.
11. Shimizu, H., Shargill, N.S., Bray, G.A., Yen, T.T., and Gesellchen, P.D. 1989. Effects of MSH on food intake, body weight and coat color of the yellow obese mouse. *Life Sci.* **45**:543–552.
12. Fan, W., Boston, B.A., Kesterson, R.A., Hruby, V.J., and Cone, R.D. 1997. Role of melanocortinergic neurons in feeding and the agouti obesity syndrome. *Nature.* **385**:165–168.
13. Thiele, T.E., et al. 1998. Central infusion of melanocortin agonist MTII in rats: assessment of c-Fos expression and taste aversion. *Am. J. Physiol.* **274**:R248–R254.
14. Vaisse, C., Clement, K., Guy-Grand, B., and Froguel, P. 1998. A frameshift mutation in human MC4R is associated with a dominant form of obesity. *Nat. Genet.* **20**:113–114.
15. Yeo, G.S., et al. 1998. A frameshift mutation in MC4R associated with dominantly inherited human obesity. *Nat. Genet.* **20**:111–112.

16. Lubrano-Berthelier, C., Le Stunff, C., Bougneres, P., and Vaisse, C. 2004. A homozygous null mutation delineates the role of the melanocortin-4 receptor in humans. *J. Clin. Endocrinol. Metab.* **89**:2028–2032.
17. Valli-Jaakola, K., et al. 2004. Identification and characterization of melanocortin-4 receptor gene mutations in morbidly obese Finnish children and adults. *J. Clin. Endocrinol. Metab.* **89**:940–945.
18. Ma, L., Tataranni, P.A., Bogardus, C., and Baier, L.J. 2004. Melanocortin 4 receptor gene variation is associated with severe obesity in Pima Indians. *Diabetes.* **53**:2696–2699.
19. Huszar, D., et al. 1997. Targeted disruption of the melanocortin-4 receptor results in obesity in mice. *Cell.* **88**:131–141.
20. Ste Marie, L., Miura, G.I., Marsh, D.J., Yagaloff, K., and Palmiter, R.D. 2000. A metabolic defect promotes obesity in mice lacking melanocortin-4 receptors. *Proc. Natl. Acad. Sci. U. S. A.* **97**:12339–12344.
21. Marsh, D.J., et al. 1999. Response of melanocortin-4 receptor-deficient mice to anorectic and orexigenic peptides. *Nat. Genet.* **21**:119–122.
22. Haskell-Luevano, C., et al. 1999. Characterization of the neuroanatomical distribution of agouti-related protein immunoreactivity in the rhesus monkey and the rat. *Endocrinology.* **140**:1408–1415.
23. Butler, A.A., et al. 2000. A unique metabolic syndrome causes obesity in the melanocortin-3 receptor-deficient mouse. *Endocrinology.* **141**:3518–3521.
24. Chen, A.S., et al. 2000. Inactivation of the mouse melanocortin-3 receptor results in increased fat mass and reduced lean body mass. *Nat. Genet.* **26**:97–102.
25. Appleyard, S.M., et al. 2003. A role for the endogenous opioid beta-endorphin in energy homeostasis. *Endocrinology.* **144**:1753–1760.
26. Hayward, M.D., Pintar, J.E., and Low, M.J. 2002. Selective reward deficit in mice lacking beta-endorphin and enkephalin. *J. Neurosci.* **22**:8251–8258.
27. Jackson, E., Stolz, D., and Martin, R. 1976. Effect of adrenalectomy on weight gain and body composition of yellow obese mice (Ay/a). *Horm. Metab. Res.* **8**:452–455.
28. Makimura, H., et al. 2000. Adrenalectomy reverses obese phenotype and restores hypothalamic melanocortin tone in leptin-deficient ob/ob mice. *Diabetes.* **49**:1917–1923.
29. Shimomura, Y., Bray, G.A., and Lee, M. 1987. Adrenalectomy and steroid treatment in obese (ob/ob) and diabetic (db/db) mice. *Horm. Metab. Res.* **19**:295–299.
30. Shimizu, H., Shargill, N.S., and Bray, G.A. 1989. Adrenalectomy and response to corticosterone and MSH in the genetically obese yellow mouse. *Am. J. Physiol.* **256**:R494–R500.
31. Bray, G.A., Stern, J.S., and Castonguay, T.W. 1992. Effect of adrenalectomy and high-fat diet on the fatty Zucker rat. *Am. J. Physiol.* **262**:E32–E39.
32. Freedman, M.R., Horwitz, B.A., and Stern, J.S. 1986. Effect of adrenalectomy and glucocorticoid replacement on development of obesity. *Am. J. Physiol.* **250**:R595–R607.
33. Mayo-Smith, W., et al. 1989. Body fat distribution measured with CT: correlations in healthy subjects, patients with anorexia nervosa, and patients with Cushing syndrome. *Radiology.* **170**:515–518.
34. Hochgeschwender, U., Costa, J.L., Reed, P., Bui, S., and Brennan, M.B. 2003. Altered glucose homeostasis in POMC null mouse mutants lacking central and peripheral melanocortin. *Endocrinology.* **144**:5194–5202.
35. Rubinstein, M., Mortrud, M., Liu, B., and Low, M.J. 1993. Rat and mouse proopiomelanocortin gene sequences target tissue-specific expression to the pituitary gland but not to the hypothalamus of transgenic mice. *Neuroendocrinology.* **58**:373–380.
36. Low, M., Rubinstein, M., and Chan, E. 2001. Transgenic analysis of the proopiomelanocortin neuroendocrine system. In *Transgenics in endocrinology*. M. Matzuk, C. Brown, and R. Kumar, editors. Humana Press. Totowa, New Jersey, USA. 319–337.
37. Pace, N., Rahlmann, D.F., and Smith, A.H. 1980. Scaling of metabolic rate on body mass in small laboratory mammals. *Physiologist.* **23**(Suppl. 6):S115–S116.
38. Elia, M., and Livesey, G. 1992. Energy expenditure and fuel selection in biological systems: the theory and practice of calculations based on indirect calorimetry and tracer methods. *World Rev. Nutr. Diet.* **70**:68–131.
39. Challis, B.G., et al. 2004. Mice lacking pro-opiomelanocortin are sensitive to high-fat feeding but respond normally to the acute anorectic effects of peptide-YY(3-36). *Proc. Natl. Acad. Sci. U. S. A.* **101**:4695–4700.
40. Masuzaki, H., et al. 2001. A transgenic model of visceral obesity and the metabolic syndrome. *Science.* **294**:2166–2170.
41. Cnop, M., et al. 2002. The concurrent accumulation of intra-abdominal and subcutaneous fat explains the association between insulin resistance and plasma leptin concentrations: distinct metabolic effects of two fat compartments. *Diabetes.* **51**:1005–1015.
42. Coll, A.P., Farooqi, I.S., Challis, B.G., Yeo, G.S., and O'Rahilly, S. 2004. Proopiomelanocortin and energy balance: insights from human and murine genetics. *J. Clin. Endocrinol. Metab.* **89**:2557–2562.
43. Machinal, F., Dieudonne, M.N., Leneveu, M.C., Pecquery, R., and Giudicelli, Y. 1999. In vivo and in vitro ob gene expression and leptin secretion in rat adipocytes: evidence for a regional specific regulation by sex steroid hormones. *Endocrinology.* **140**:1567–1574.
44. Anderson, L.A., McTernan, P.G., Barnett, A.H., and Kumar, S. 2001. The effects of androgens and estrogens on preadipocyte proliferation in human adipose tissue: influence of gender and site. *J. Clin. Endocrinol. Metab.* **86**:5045–5051.
45. Dos Santos, E.G., et al. 2002. Rapid nongenomic E2 effects on p42/p44 MAPK, activator protein-1, and cAMP response element binding protein in rat white adipocytes. *Endocrinology.* **143**:930–940.
46. Weide, K., et al. 2003. Hyperphagia, not hypometabolism, causes early onset obesity in melanocortin-4 receptor knockout mice. *Physiol. Genomics.* **13**:47–56.
47. De Vos, P., Saladin, R., Auwerx, J., and Staels, B. 1995. Induction of ob gene expression by corticosteroids is accompanied by body weight loss and reduced food intake. *J. Biol. Chem.* **270**:15958–15961.
48. Considine, R.V. 2001. Regulation of leptin production. *Rev. Endocr. Metab. Disord.* **2**:357–363.
49. Kahn, B.B., and Flier, J.S. 2000. Obesity and insulin resistance. *J. Clin. Invest.* **106**:473–481.
50. Shuldiner, A.R., Yang, R., and Gong, D.W. 2001. Resistin, obesity and insulin resistance: the emerging role of the adipocyte as an endocrine organ. *N. Engl. J. Med.* **345**:1345–1346.
51. Zakrzewska, K.E., Cusin, I., Sainsbury, A., Rohner-Jeanrenaud, F., and Jeanrenaud, B. 1997. Glucocorticoids as counterregulatory hormones of leptin: toward an understanding of leptin resistance. *Diabetes.* **46**:717–719.
52. Drazen, D.L., et al. 2003. Adrenalectomy alters the sensitivity of the central nervous system melanocortin system. *Diabetes.* **52**:2928–2934.
53. Freedman, M.R., Castonguay, T.W., and Stern, J.S. 1985. Effect of adrenalectomy and corticosterone replacement on meal patterns of Zucker rats. *Am. J. Physiol.* **249**:R584–R594.
54. Castonguay, T.W. 1991. Glucocorticoids as modulators in the control of feeding. *Brain Res. Bull.* **27**:423–428.
55. Makimura, H., Mizuno, T.M., Beasley, J., Silverstein, J.H., and Mobbs, C.V. 2003. Adrenalectomy stimulates hypothalamic proopiomelanocortin expression but does not correct diet-induced obesity. *BMC Physiol.* **3**:4. doi:10.1186/1472-6793-3-4.
56. Green, P.K., Wilkinson, C.W., and Woods, S.C. 1992. Intraventricular corticosterone increases the rate of body weight gain in underweight adrenalectomized rats. *Endocrinology.* **130**:269–275.
57. Zakrzewska, K.E., et al. 1999. Induction of obesity and hyperleptinemia by central glucocorticoid infusion in the rat. *Diabetes.* **48**:365–370.
58. Sainsbury, A., Wilks, D., and Cooney, G.J. 2001. Central but not peripheral glucocorticoid infusion in adrenalectomized male rats increases basal and substrate-induced insulinemia through a parasympathetic pathway. *Obes. Res.* **9**:274–281.
59. Kellendonk, C., et al. 2002. Inactivation of the GR in the nervous system affects energy accumulation. *Endocrinology.* **143**:2333–2340.
60. Stenzel-Poore, M.P., Cameron, V.A., Vaughan, J., Sawchenko, P.E., and Vale, W. 1992. Development of Cushing's syndrome in corticotropin-releasing factor transgenic mice. *Endocrinology.* **130**:3378–3386.
61. Low, M.J., et al. 2001. Somatostatin is required for masculinization of growth hormone-regulated hepatic gene expression but not of somatic growth. *J. Clin. Invest.* **107**:1571–1580.
62. Spiegelman, B.M., and Flier, J.S. 2001. Obesity and the regulation of energy balance. *Cell.* **104**:531–543.
63. Pung, T., Zimmerman, K., Klein, B., and Ehrich, M. 2003. Corticosterone in drinking water: altered kinetics of a single oral dose of corticosterone and concentrations of plasma sodium, albumin, globulin, and total protein. *Toxicol. Ind. Health.* **19**:171–182.
64. Chisari, A.N., Perone, M.J., Giovambattista, A., and Spinedi, E. 1998. Gender-dependent characteristics of the hypothalamo-corticotrope axis function in glucocorticoid-replete and glucocorticoid-depleted rats. *J. Endocrinol. Invest.* **21**:737–743.
65. Bluher, S., et al. 2004. Responsiveness to peripherally administered melanocortins in lean and obese mice. *Diabetes.* **53**:82–90.
66. Forbes, S., Bui, S., Robinson, B.R., Hochgeschwender, U., and Brennan, M.B. 2001. Integrated control of appetite and fat metabolism by the leptin-proopiomelanocortin pathway. *Proc. Natl. Acad. Sci. U. S. A.* **98**:4233–4237.
67. Pierroz, D.D., et al. 2002. Effects of acute and chronic administration of the melanocortin agonist MTII in mice with diet-induced obesity. *Diabetes.* **51**:1337–1345.
68. Cettour-Rose, P., and Rohner-Jeanrenaud, F. 2002. The leptin-like effects of 3-d peripheral administration of a melanocortin agonist are more marked in genetically obese Zucker (fa/fa) than in lean rats. *Endocrinology.* **143**:2277–2283.
69. Hamilton, B.S., and Doods, H.N. 2002. Chronic application of MTII in a rat model of obesity results in sustained weight loss. *Obes. Res.* **10**:182–187.
70. Trivedi, P., et al. 2003. Exploring the site of anorectic action of peripherally administered synthetic melanocortin peptide MT-II in rats. *Brain Res.* **977**:221–230.
71. Smart, J.L., and Low, M.J. 2003. Lack of proopiomelanocortin peptides results in obesity and defective adrenal function but normal melanocyte pigmentation in the murine C57BL/6 genetic background. *Ann. N. Y. Acad. Sci.* **994**:202–210.